Journal of Cellular Biochemistry 100:112–128 (2007)

Phosphatidic Acid Regulates the Affinity of the Murine Phosphatidylinositol 4-phosphate 5-kinase-Iβ for Phosphatidylinositol-4-phosphate

Marta Jarquin-Pardo, Abbie Fitzpatrick, Floyd J. Galiano, Eric A. First, and J. Nathan Davis*

Feist-Weiller Cancer Center and Department of Biochemistry and Molecular Biology, Louisiana State University Health Sciences Center, 1501 Kings Highway, Shreveport Louisiana 71130-3932

Abstract Type I phosphatidylinositol 4-phosphate 5-kinase (PI4P5K) catalyzes the phosphorylation of phosphatidylinositol 4 phosphate [PI(4)P] at carbon 5, producing phosphatidylinositol 4,5 bisphosphate [PI(4,5)P2]. Phosphatidic acid (PA) activates PI4P5K in vitro and plays a central role in the activation of PIP5K pathways in vivo. This report demonstrates that actin fiber formation in murine fibroblasts involves PA activation of PIP5Ks and defines biochemical interactions between PA and the PIP5Ks. Inhibition of phospholipase D production of PA results in the loss of actin fibers. Overexpression of the beta isoform of the type I murine phosphatidylinositol 4-phosphate 5-kinase (mPIP5K-Iβ) maintains actin fiber structure in the face of phospholipase D inhibition. PA activates mPIP5K-Iβ by direct binding to mPIP5K-Iβ through both electrostatic and hydrophobic interactions, with the fatty acid acyl chain length and degree of saturation acting as critical determinants of binding and activation. Furthermore, kinetic analysis suggests that phosphorylation of the PI(4)P substrate does not follow classical Michaelis–Menten kinetics. Instead, the kinetic data are consistent with a model in which mPIP5K-Iβ initially binds to the lipid micelle and subsequently binds the PI(4)P substrate. In addition, the kinetics indicate substrate inhibition, suggesting that mPIP5K-Iβ contains an inhibitory PI(4)P-binding site. These results suggest a model in which mPIP5K-Iβ is surrounded by PI(4)P, but is unable to catalyze its conversion to PI(4,5)P2 unless PA is bound. J. Cell. Biochem. 100: 112–128, 2007.

Key words: phosphatidic acid; type I phosphatidylinositol 4-phosphate 5-kinase; PIP Kinase; phosphatidylinositol 4,5 bisphosphate

Phosphatidylinositol metabolism regulates diverse and essential cellular processes including signal transduction, membrane trafficking, gene expression, energy metabolism, macromolecular synthesis, and dynamic control of cytoskeletal structure, reviewed by Doughman et al. [2003a] and Oude Weernink et al. [2004]. The type I PI4P5Ks lie at a nexus within phosphatidylinositol pathways since it catalyzes formation of the two major regulatory phosphatidylinositides, PI(4,5)P2 and PI(3,4,5)P3 (phosphatidylinositol 3,4,5 trisphosphate).

The type I PI4P5Ks are encoded by a small gene family comprising three genes (α, β , and γ) each of which produces multiple isoforms via selective RNA processing [Ishihara et al., 1996, 1998; Loijens and Anderson, 1996; Loijens et al., 1996; Itoh et al., 1998]. While these three genes may have overlapping biological roles, isoform specific functions have been associated with the products of each gene. For example, murine PIP5K-Iβ (human PIP5K-Iα) has been

Abbreviations used: PI4P5K, phosphatidylinositol 4-phosphate 5-kinase; PI(4,5)P2, phosphatidylinositol 4,5 bisphosphate; PA, phosphatidic acid;mPIP5K-Iβ, murine phosphatidylinositol 4-phosphate 5-kinase type I beta; PI(4)P, phosphatidylinositol 4-phosphate; PI(3,4,5)P3, phosphatidylinositol 3,4,5 trisphosphate; IP3, inositol trisphosphate; ARF, ADP-ribosylation factor; GST, glutathione-S-transferase; PCR, polymerase chain reaction; CSF-1R, colony stimulating factor-1 receptor; GFP, green fluorescent protein; DIC, differential interference microscopy; ELISA, enzyme linked immunosorbent assay; DAG, diacylglycerol; DMPA, dimyristoyl-sn-glycero-3-phosphate; DPPA, dipalmityl-sn-glycero-3-phosphate; DLPA, dilinoleoyl-sn-glycero-3-phosphate.

Grant sponsor: National Science Foundation; Grant numbers: 9992410, 0235028.

*Correspondence to: J. Nathan Davis, Department of Biochemistry and Molecular Biology, Louisiana State University Health Sciences Center, P.O. Box 33932, Shreveport, LA. 71130-3932. E-mail: ndavis@lsuhsc.edu

Received 19 April 2006; Accepted 17 May 2006

DOI 10.1002/jcb.21027

implicated in the trafficking and signaling of receptor tyrosine kinases, mRNA metabolism, phagocytosis, and membrane ruffling [Davis et al., 1997; Boronenkov et al., 1998; Barbieri et al., 2001; Doughman et al., 2003b]. PIP5K-Iγ regulates synaptic vesicle trafficking, focal adhesions, and IP3 /Ca^{2+} signaling downstream of G-protein coupled receptors [Wenk et al., 2001; Di Paolo et al., 2002, 2004; Ling et al., 2002; Wang et al., 2004]. Murine PIP5K-Iα (human PIP5K-Iβ) has been less well characterized but displays perinuclear membrane staining [Doughman et al., 2003b]. Thus, precise control of PI(4,5)P2 production likely derives in part from isoform-specific functions involving unique targeting domains.

While regulated expression and specific targeting are important regulatory mechanisms, other mechanisms are employed to regulate the PIP5Ks. Phosphorylation of the PIP5Ks is an important mechanism of control for PI(4,5)P2-dependent pathways [Park et al., 2001; Ling et al., 2002; Doughman et al., 2003a; Oude Weernink et al., 2004]. Association with G-proteins also regulates the PIP5K activity. The Rho family of small GTPases (Rho, Rac, and Cdc42) regulates PI(4,5)P2 production in a number of biological settings via multiple mechanisms that are all dependent upon PIP5Ks [Chatah and Abrams, 2001; Weernink et al., 2004; Yang et al., 2004], reviewed by Oude Weernink et al. [2004]) and the ADP-ribosylation factor (ARF) family of GTPases has also been implicated in PIP5K-dependent regulation of membrane trafficking and dynamics, regulated secretion, and actin cytoskeleton regulation [Honda et al., 1999; Brown et al., 2001; Aikawa and Martin, 2003].

While post-translational modification and protein interactions are important regulatory factors for the PIP5Ks, membrane lipids also play key regulatory roles. Early studies with purified type I PIP5Ks demonstrated direct stimulation of PIP5K activity by phosphatidic acid (PA) [Moritz et al., 1992; Jenkins et al., 1994] and later PA and PI(4,5)P2 were shown to co-regulate biological processes such as endocytosis and actin polymerization [Cross et al., 1996; Arneson et al., 1999; Kam and Exton, 2001; Yin and Janmey, 2003]. The observation that ARF GTPases regulate both phospholipase D enzymes and PIP5Ks together with evidence that PA and PI(4,5)P2 regulate overlapping cellular functions suggests that an intimate connection exists between these enzyme families [Honda et al., 1999; Brown et al., 2001; Skippen et al., 2002]. Consistent with this notion, PIP5K-Iα directly associates with both phospholipase D1 and phospholipase D2 and recruits phospholipase D2 to intracellular vesicles [Divecha et al., 2000]. Additionally, ARF1 mutants that fail to bind phospholipase D do not enhance PI(4,5)P2 production in vivo as effectively as wild-type ARF1 [Skippen et al., 2002]. While these and other studies find consistent biological links between PA and PI(4,5)P2 production, an examination of the biochemistry underlying the PA stimulation of PIP5Ks is lacking. Thus, the research detailed in this report was undertaken to elucidate the structural and biochemical interactions between mPIP5K-Iβ and PA.

In the present study, the biological, physical, and biochemical interactions between mPIP5K-Iβ and PA are examined. mPIP5K-Iβ directly binds PA through both charge and lipid interactions. PA binding by mPIP5K-Iβ is dependent upon acyl chain length while PA-activation of mPIP5K-Iβ kinase activity also requires that the fatty acid chains be unsaturated. PA significantly enhanced the affinity of mPIP5K-Iβ for PI(4)P with minimal effects on the overall rate of the reaction. Interestingly, substrate inhibition of mPIP5K-Iβ activity is observed by PI(4)P and PA had only a small effect on this substrate inhibition.

MATERIALS AND METHODS

Materials

Ninety-six-well microtiter plates were obtained from Becton Dickinson. Glutathione Sepharose 4B was purchased from Amersham Pharmacia Biotech. Rabbit polyclonal antibody directed against Glutathione-S-Transferase (GST) was purchased from Sigma. Reduced glutathione was obtained from Fisher Scientific. The phospholipids used in the binding experiments were obtained from the following companies: 1,2-dipalmitoyl-rac-glycerol (Sigma); dipalmitoyl phosphatidylinositol-(3,4,5)-trisphosphate (Matreya); phosphatidic acid (Sigma); phosphatidylinositol-4-phosphate; 1,2-dioctanoyl-sn-glycero-3-phosphate; 1-myristoyl-2-hydroxy-*sn*-glycero-3-phosphate, 1,2-dimyristoyl-sn-glycero-3-phosphate; 1,2-dipalmityl-sn-glycero-phospahte; 1,2, distearoyl-sn-glycero-3-phosphate; dilinoleoyl-sn-glycero-3-phosphate, 1,2-diarachidonoyl-sn-glycero-3-phosphate; and phosphatidy-

linositol- (4,5)-bisphosphate (Avanti Polar Lipids). To study the effects of phosphatidic acid on the activity of the mPIP5K-Iβ, dipalmitoyl phosphatidylinositol-4-phosphate (Echelon) was used as a substrate. The respective GST fusion proteins were purified from *E. coli* XL-1 blue host cells. GST-mPIP5K-Iβ used in this study was previously described [Galiano et al., 2002].

Visualization of Actin in NIH-3T3 Cells

NIH-3T3 CSF-1R cells were transfected with pcDNA GFP-mPIP5K-Iβ and pHygro and selected in complete DMEM supplemented with 400 μg/ml neomycin and 100 μg/ml hygromycin. After 2 weeks, the GFP-expressing cells were enriched by two rounds cell sorting based upon GFP fluorescence using a FACSVantage SE (BD Biosciences). The expression of GFP-mPIP5K-Iβ was confirmed by immunoprecipitation with anti-mPIP5K-Iβ antiserum. The actin cytoskeleton was stained using the actin cytoskeleton and focal adhesion staining kit (Chemicon International, Temecula, CA). The cells were washed, fixed with paraformaldehyde, and F-actin stained with rhodamine-phalloidin. DIC and fluorescence images were obtained with an Olympus-AX-70 epifluorescence microscope equipped with differential interference optics. Monochrome images were captured at the microscope using a cooled-CCD camera (Nu 200: Princeton Instruments) and IP-Lab software (Scanalytics, Inc.) run on an Apple G4 computer.

Preparation of Pellet and Soluble Fractions From NIH 3T3 Cells Treated With 1-butanol

NIH 3T3 cells were plated (8×10^6 cells) on 100-mm dishes and after 24 h, the medium was replaced with 12 ml of DMEM containing either 1-butanol or 2-butanol (0.5% v/v). After 1 h, the medium was removed and the cells were scraped on ice in 10 ml of buffer (10 mM Tris pH 7.5, 1 mM EDTA, 1 mM EGTA), pelleted by centrifugation, and resuspended in 1.5 ml of homogenizing buffer (10 mM Tris pH 7.5, 20 mM NaCl). After incubation on ice for 30 min, the cells were Dounce-homogenized (40 strokes) and passed through a 25G needle (25–30 passes). Nuclei and unbroken cells were removed by centrifugation at 2500 rpm for 10 min at 4°C. The pellet was resuspended in 1.5 ml of homogenizing buffer and the lysis procedure repeated. The post nuclear lysates were combined and the membrane fraction obtained after centrifugation at 1,00,000*g* (28,800 rpm in a SW50.1 Beckman rotor) for 1 h at 4°C. The soluble fraction was collected and the membrane pellet was resuspended by sonication in 1.5 ml of buffer containing 10 mM Tris pH 7.5, 1% Triton X-100, 500 mM NaCl.

Immunoprecipitation of Endogenous mPIP5K-Iβ From NIH 3T3 Cells

Soluble and pellet fractions from NIH 3T3 cells were freshly prepared as described above. For each immunoprecipitation, 60 μg of protein in equal volume (1.5 ml) IP buffer (25 mM Tris pH 7.5, 100 mM NaCl, and 0.1% Triton X-100) was immunoprecipitated with a polyclonal antibody against the mPIP5K-Iβ (7 μl) and Sepharose-6B-coupled protein A. The protein-A beads were collected by brief centrifugation and washed six times with the following buffers: 1× IP kinase buffer (25 mM Tris pH 7.5, 100 mM NaCl, 0.1% Triton X-100); 1× PBS pH 6.0, 0.5% Triton X-100; 1× 25 mM Tris pH 8, 100 mM NaCl, 0.1% Triton X-100; 1× with 25 mM Tris pH 7.5, 500 mM NaCl, 0.1% Triton X-100; and 2× with IP kinase buffer. The immunoprecipitates were used in a kinase assay as described below.

Expression and Purification of the GST-PIP5K-Iβ Fusion Proteins

Overnight cultures were diluted 1:10 in Luria Broth; after 2 h, GST-fusion protein expression was induced with 2 mM IPTG. After 1 h, the cells were collected by centrifugation, resuspended in lysis buffer (PBS, 0.5% Tween 20), and lysed by sonication. The lysates were clarified by centrifugation and incubated with glutathione Sepharose at 4°C for 1 h. The beads were collected by centrifugation, washed 3× in lysis buffer, and the protein was eluted in 50 mM Tris pH 8, 20 mM reduced glutathione.

ELISA Phospholipid-Binding Assay

The previously described ELISA phospholipid-binding assay [Ghosh et al., 1996] was adapted to study the interaction of the different GST-mPIP5K-Iβ fusion proteins with phosphatidic acid. All procedures were performed at room temperature. Two micrograms of each phospholipid were diluted in methanol, added to a well in a 96-well microtiter plate, and allowed to bind overnight. The plates were blocked with 3% fatty acid free bovine serum albumin (BSA,

Boeringher Mannheim) in TTBS buffer (10 mM Tris pH 7.5, 150 mM NaCl, 0.1% Tween 20) for 1 h. Glutathione-S-transferase (GST)-fusion proteins were added in dilution buffer (0.3% BSA in TTBS) and incubated for 1 h. The plate was washed with TTBS and anti-GST rabbit polyclonal antiserum (1:2,000 dilution in dilution buffer) was added and incubated for 1 h. The plate was washed in TTBS and the secondary antibody (1:2,000 dilution of goat anti-rabbit IgG-alkaline phosphatase conjugate, Bio-Rad) was added and incubated for 1 h. The plate was washed as before and 150 μl of a 10 mg/ml solution of 4-nitrophenyl phosphate (Amaresco) in substrate buffer (10 mM Tris-HCl, pH 9.5, 100 mM NaCl, 5 mM $MgCl_2$) was added to each well. After 25 min, the absorbance at 405 nm was measured on an ELISA plate reader (Bio-Rad). For the competition experiments, the GST-fusion proteins were preincubated with the competitors for 30 min.

Purification of GST-mPIP5K-Iβ From 293T Cells

GST-mPIP5K-Iβ was purified from cell lysate prepared from transiently transfected 293T cells. pcDNA3 GST-mPIP5K-Iβ was constructed by digestion of pGEX-2T-mPIP5K-Iβ with Ace I and Xho I. The Ace I site was end-filled and the fragment ligated to EcoRV and Xho I digested pcDNA III. Transient transfection was performed using the modified calcium phosphate method and 293T cells (2×10^7 cells/150 mm dish, 20 plates/experiment). At 16–20 h, the cells were scraped, collected by centrifugation, suspended in 50 ml TBST (10 mM Tris pH 7.4, 150 mM NaCl, 0.5% Triton X-100), and lysed by trituration. The lysate was clarified by centrifugation in Sorvall SA600 rotor (10,000 rpm for 20 min), the supernatant collected, and the pellet-associated enzyme was released by resuspension of the pellet in 10 ml TBST adjusted to 500 mM NaCl and suspended by Dounce homogenization. The pellet wash was clarified as above, the supernatants combined, and 0.2 ml of a 50% slurry of GST-Sepharose was added and incubated at 4°C for 1 h with constant agitation. The bound protein was washed three times with 50 ml TBST, 1 time with 50 ml PBS pH 6.0, and 1 time with 50 ml TBST, and the protein eluted by addition of two aliquots of 0.1 ml elution buffer (50 mM Tris pH 8.0, 120 mM NaCl, 20 mM reduced glutathionine).

Kinase Assays

GST-mPIP5K-Iβ purified from 293T cells was used in all kinase reactions. All kinase reactions were performed in a 50 μl reaction volume at room temperature in standard buffer, which contained 50 mM Tris-Cl pH 7.5, 1 mM EGTA, 10 mM $MgCl_2$, 100 mM NaCl, 0.1% Triton, X-100, and 50 μM [γ-^{32}P]ATP (10 μCi/reaction). The reactions were quenched after 5 min by the addition of 200 μl of 1N HCl. Phospholipids were extracted with 600 μl of chloroform: methanol:(12N) HCl (200:100:1). The organic phase was separated by centrifugation (5 min), dried in a speed vacuum centrifuge, and resuspended in 100 μl of chloroform: methanol:(12N)HCl (200:100:1). One-fourth of the organic phase (25 μl) was spotted onto a thin layer chromatography (TLC) plate. Immediately prior to use, TLC plates were coated with a solution of methanol:water (40:60) containing 1% $K_2C_2O_4$ and 1 mM EGTA. TLC-coated plates were activated by heating at 100°C for 20 min, and phospholipids separated by developing in chloroform:acetone:methanol:acetic acid: water (46:17:15:14:8). After separation, the [^{32}P]-labeled phospholipids were visualized by autoradiography followed by analysis on a phosphorimager. Standard non-radioactive phospholipids (PI(4)P, PI(4,5)P2 and phosphatidic acid) were stained with primuline and visualized on a UV transilluminator. After primuline staining, the area containing [^{32}P]PI(4,5)P2 was located and excised based on the migration of the non-radioactive PI(4,5)P2 standard. Excised [^{32}P]PI(4,5)P2 was counted by scintillation counting in 2 ml of ScintiVerseI. For all experiments, GST-PIP5KI-β was added to a final concentration of 5 nM. In the studies of the PI(4)P dependence of PI(4,5)P2 production, PI(4)P concentration was varied from 2.5 to 250 μM, and phosphatidic acid was added to a final concentration of 100 μM. All assays were performed in the linear range with regard to the enzyme concentration and incubation time.

Kinetic Analyses

The kinetic data were plotted as a function of PI(4)P total concentration (Case I) and PI(4)P effective surface concentration (Case II). In Case I, the data were fit to the Hill equation modified for uncompetitive substrate

inhibition:

$$v = \frac{v_{max}[PI(4)P_o]^n}{\left(K_m^{PI(4)P}\right)^n + [PI(4)P_o]^n + \frac{[PI(4)P_o]^{n+1}}{K_i^{PI(4)P}}} \quad (1)$$

where V_{max} is the maximal rate for PI(4,5)P2 production, $[PI(4)P_0]$ is the total PI(4)P concentration, $K_m^{PI(4)P}$ is the Michaelis constant of PI(4)P, $K_i^{PI(4)P}$ is the Michaelis constant of PI(4)P at the inhibitory site, and n is the Hill coefficient. For case II, the data were fit to the Michaelis-Menten equation modified for uncompetitive substrate inhibition:

$$v = \frac{\left(\frac{v_{max}}{1 + \frac{[PI(4)P_e]}{K_i^{PI(4)P_e}}}\right)[PI(4)P_e]}{\left(\frac{K_m^{PI(4)P_e}}{1 + \frac{[PI(4)P_e]}{K_i^{PI(4)P_e}}}\right) + [PI(4)P_e]} \quad (2)$$

where V_{max} is the maximal rate for PI(4,5)P2 production, $[PI(4)P_e]$ is the effective surface concentration of PI(4)P, $K_m^{PI(4)P_e}$ is the Michaelis constant for the dissociation of PI(4)P from the active site, and $K_i^{PI(4)P_e}$ is the Michaelis constant for the dissociation of PI(4)P from the inhibitory site. To determine the effective surface concentration of PI(4)P, the mole fraction of PI(4)P at the surface of the micelle was multiplied by the total concentration of PI(4)P:

$$[PI(4)P_e] = \left(\frac{[PI(4)P_o]}{[PI(4)P_o] + [PA_o] + [TritonX - 100]}\right) \times [PI(4)P_o] \quad (3)$$

where $[PI(4)P_0]$ is the total concentration of PI(4)P, $[PA_0]$ is the total concentration of phosphatidic acid and [Triton X-100] is the concentration of Triton X-100. For analysis of the phosphatidic acid dependence of PI(4,5)P2 production, the phosphatidic acid concentration was varied from 5 to 200 μM and PI(4)P was added to a final concentration of 65 μM. The kinetic data were plotted as a function of the effective surface concentration of phosphatidic acid and fit to the Hill equation:

$$v = \frac{V_{max}[PA_e]^n}{(K_m^{PA_e})^n + [PA_e]^n} \quad (4)$$

where V_{max} is the maximal rate of PI(4,5)P2 production, $K_m^{PA_e}$ is the Michaelis constant for phosphatidic acid, n is the Hill coefficient, and $[PA_e]$ is the effective surface concentration of phosphatidic acid. The effective surface concentration of phosphatidic acid was determined using the following equation:

$$[PA_e] = \left(\frac{[PI(4)P_o]}{[PI(4)P_o] + PA_o] + [TritonX - 100]}\right) \times [PA_o] \quad (5)$$

where $[PA_0]$ is the total concentration of phosphatidic acid, $[PI(4)P_0]$ is the total concentration of PI(4)P, and [TritonX-100] is the total concentration of TritonX-100.

Cell Lines

293T and NIH 3T3 cells were grown in Dulbecco's modification of minimal essential media (DMEM; Cellgro) supplemented with 10% fetal bovine serum (Biowhittaker), 100 U of penicillin/streptomycin (Cellgro), and maintained at 37°C in an atmosphere of 5% CO_2. Cells were transfected by using a modified calcium phosphate precipitation procedure as previously described [Chen and Okayama, 1987].

RESULTS

mPIP5K-Iβ and Phosphatidic Acid Collaborate in Actin Stress Fiber Formation

Since PA and PI(4,5)P2 positively regulate actin fiber formation and the kinase activity of the type I PIP5Ks is stimulated in vitro by PA, we hypothesized that PA regulation of actin polymerization is mediated through activation of the type I PIP5Ks. To test this hypothesis, the effect of inhibiting phospholipase D-derived PA production on actin fiber formation was determined in parental NIH 3T3 cells and NIH 3T3 cells engineered to express GFP-mPIP5K-Iβ. We expected that increased expression of mPIP5K-Iβ could substitute for PA-activation of the endogenous levels of mPIP5K-Iβ and support actin polymerization in the absence of PA. Parental and GFP-mPIP5K-Iβ-expressing NIH-3T3 cells demonstrated intact and well-organized actin filaments after phalloidin staining (Fig. 1A, top panels). Since in the presence of primary alcohols, phospholipase D

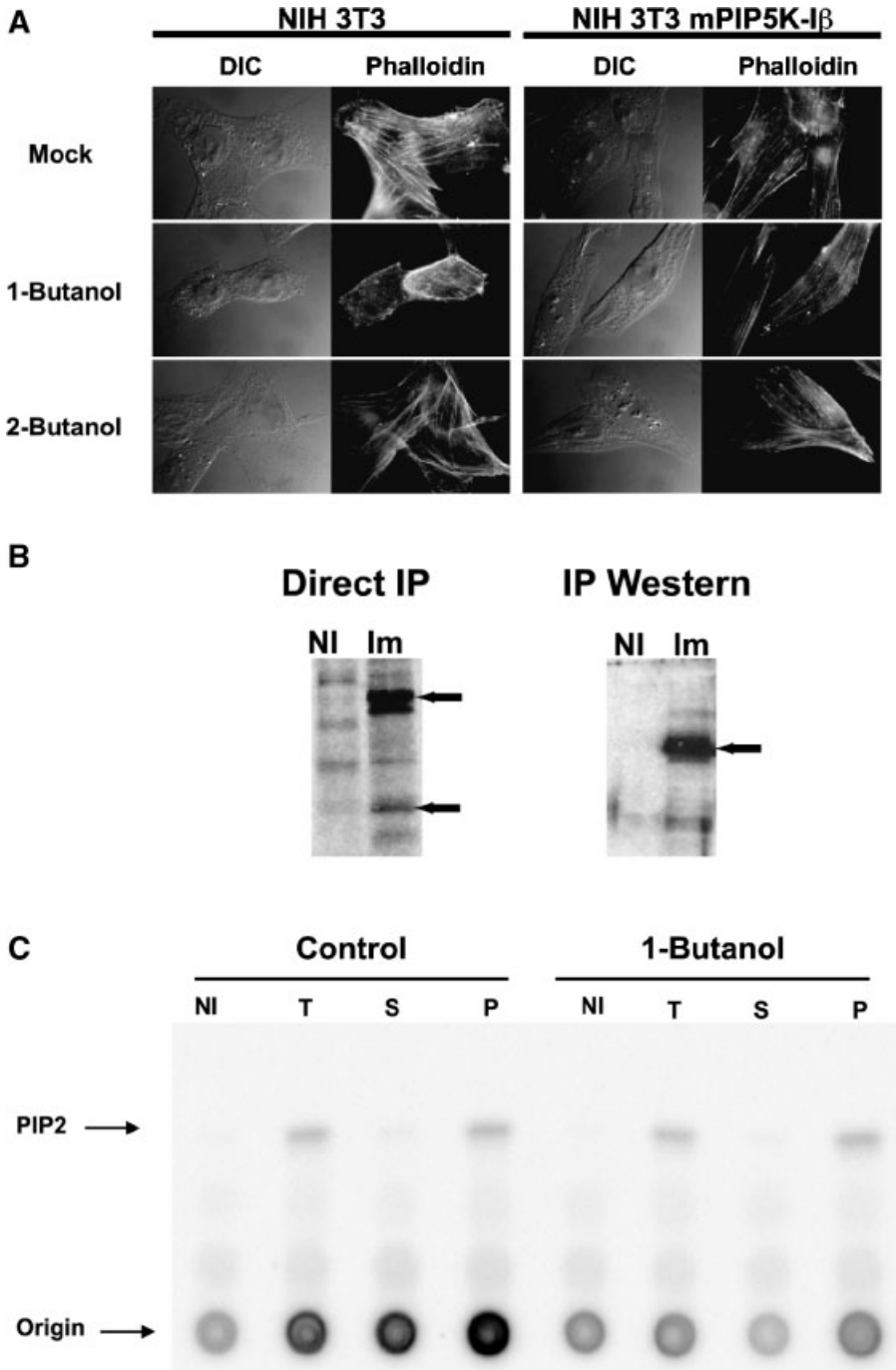

Fig. 1. GFP-mPIP5K-Iβ expression supports actin fiber formation in the face of inhibition of PLD dependent production of PA. **Panel A** shows photomicrographs obtained by using differential interference contrast microscopy (DIC) or fluorescent microscopy (Phalloidin) of parental NIH 3T3 cells (**left panels** as indicated) or NIH 3T3 cells expressing GFP-mPIP5K-Iβ (**right panels**, as indicated) stained with rhodamine-phalloidin. PLD synthesis of PA was inhibited by the addition of 0.5% 1-butanol (**center panels**, as indicated). As a control for the alcohol effects on the cells, addition of 0.5% 2-butanol was performed (**bottom panels**, as indicated). **Panel B** is an autoradiogram of proteins immunoprecipitated with non-immune serum (NI) antiserum specific for mPIP5K-Iβ (Im) from lysates prepared from ^{35}S-methionine-labeled GFP-mPIP5K-Iβ-expressing cells (**left panel**, designated Direct IP). The arrows indicate the slower migrated GFP-mPIP5K-Iβ (upper arrow)? and endogenous mPIP5K-Iβ (lower arrow). The right panel, designated IP Western, is an autoradiogram of a Western blot using the mPIP5K-Iβ specific serum and proteins immunoprecipitated from lysates prepared from the GFP-mPIP5K-Iβ-expressing cells using either non-immune serum (NI) or anti-GFP antibodies. The band corresponding to GFP-mPIP5K-Iβ is indicated by the arrow. **Panel C** is an autoradiogram of thin layer chromatography of phospholipid products formed by mPIP5K-Iβ kinase activity present in soluble or insoluble cellular fractions of control and 1-butanol treated NIH 3T3 cells as measured by immune complex kinase assays. Proteins were immunoprecipitated with either non-immune serum (NI) or serum specific for mPIP5K-Iβ. Immunoprecipitations were performed using total cellular protein (T) in cell extracts or the soluble (S) and pellet (P) fractions were prepared from parental cells treated with 0.5% 1-butanol or mock treated.

mediates a transphosphatidylation reaction that produces phosphatidyl-alcohol in lieu of PA, 1-butanol was employed to inhibit phospholipase D-mediated production of PA. Secondary alcohols are not utilized by phospholipase D and 2-butanol treatment of the cells served as a control. Thirty-minute treatment of 1-butanol resulted in dramatic loss of actin filaments in the parental NIH 3T3 cells with a concomitant rounding of the cells (Fig. 1A, middle left panel), but no effect of 2-butanol was observed (Fig. 1A, lower left panel). Expression of GFP-mPIP5K-Iβ was confirmed in the cells by direct immunoprecipation (IP) and IP-Western analysis (Fig. 1B). The GFP-mPIP5K-Iβ-expressing cells displayed normal actin filaments in the presence of both 1-butanol and 2-butanol (Fig. 1A, right middle and lower panels). Thus, inhibition of phospholipase D-mediated production of PA was required to maintain actin stress fiber integrity and mPIP5K-Iβ overexpression obviated this PA requirement. Given that PA is known to potently activate kinase activity of the type I mPIP5Ks in vitro, these results suggest that PA-dependent activation of the type I mPIP5Ks is required to maintain actin stress fibers and that expression of GFP-mPIP5K-Iβ was sufficient to substitute for the loss of PA production in the presence of 1-butanol.

Multiple mechanisms could allow PA to activate mPIP5K-Iβ including regulated recruitment to the plasma membrane, stable post-translational modification such as phosphorylation, or direct interaction with the enzyme. In order to determine if the PA production altered the membrane recruitment or overall activity of mPIP5K-Iβ, IP-kinase assays were performed using soluble and membrane fractions of lysates prepared from control and 1-butanol-treated parental NIH-3T3 cells. Interestingly, no appreciable effects were observed on total mPIP5K-Iβ enzyme activity or its subcellular localization when compared to control cells upon inhibition of PA production (Fig. 1C). Since total mPIP5K-Iβ activity was not affected by 1-butanol, a stable post-translational modification such as phosphorylation is unlikely to mediate the PA-dependent effects on mPIP5K-Iβ. Additionally, 1-butanol had no effect on the membrane localization of mPIP5K-Iβ or kinase activity suggesting that PA was not required to recruit mPIP5K-Iβ to the membrane. Thus, PA likely interacts directly with mPIP5K-Iβ and experiments designed to further characterize the PA-dependent activation of the type I PIP5Ks were undertaken.

mPIP5K-Iβ Binds to Phosphatidic Acid (PA)

While PA stimulation of the type I PIP5Ks has been shown in vitro and in vivo [Moritz et al., 1992; Jenkins et al., 1994; Divecha et al., 2000], the mechanism by which PA stimulates the type I PIP5Ks has not been studied. In vitro stimulation of type I PIP5K kinase activity together with the evidence presented above support the hypothesis that mPIP5K-Iβ is activated by the direct binding of PA to the enzyme. To test this hypothesis an ELISA based lipid-binding protocol to characterize the binding of mPIP5K-Iβ to PA was adapted from studies that examined PA-binding by the Raf-1 kinase [Ghosh et al., 1996]. Initially, the ability of mPIP5K-Iβ to bind PA, as well as, other phospholipids was examined. We reasoned that mPIP5K-Iβ would bind phosphatidylinositol-4-phosphate (PI(4)P), which is the preferred substrate of the enzyme, and phosphatidylinositol-4,5-bisphosphate (PI(4,5)P2), which is produced by mPIP5K-Iβ from PI(4)P and displays feedback inhibition on the type I PIP5Ks. Additionally, phosphatidylinositol-3, 4,5-trisphosphate (PI(3,4,5)P3), which is derived from PI(4,5)P2 by the action of a phosphatidylinositol 3-kinase (PI3K) was tested in the assay. Diacylglycerol (DAG), which does not affect type I PIP5K enzyme activity, and is not expected to bind to mPIP5K-Iβ, served as a negative control. mPIP5K-Iβ expressed in *E. coli* as a glutathione-S-transferase (GST)-fusion protein was affinity purified on glutathione-Sepharose. The wells of a 96-well titer plate were coated with the various phospholipids, and the ability of the GST-mPIP5K-Iβ to bind to the respective phospholipids was determined by ELISA (Fig. 2A). While GST-mPIP5K-Iβ bound to each phosphoinositide, albeit with varying intensities, a distinct and strong interaction of GST-mPIP5K-Iβ with PA was observed. These results support the hypothesis that PA-activation of mPIP5K-Iβ is mediated by direct binding to the enzyme.

The strong interaction between GST-mPIP5K-Iβ and PA was further characterized and titrations of protein concentration against a constant lipid amount indicated that the upper limit of the linear range of the assay was reached at 0.5 μg of GST-mPIP5K-Iβ with higher protein amounts leading to increased nonspecific binding (data

not shown). To determine whether PA binds to a specific site on GST-mPIP5K-Iβ, dose response and competition experiments were performed. Decreasing amounts of PA used in the assay resulted in reduced GST-mPIP5K-Iβ-binding, as indicated by the decrease in absorbance value with decreasing PA concentration (Fig. 2B). GST-mPIP5K-Iβ-binding was saturated at 1 μg of PA and all further experiments were performed under PA excess (2 μg of PA) to insure that GST-PIP5K-Iβ-binding was not limited by phospholipid availability.

PA, as all phospholipids, has a hydrophobic region composed of two fatty acids ester-linked to glycerol, and a charged head group. Thus, we hypothesized that specific PA-binding by mPIP5K-Iβ should involve both hydrophobic and ionic interactions. In contrast, DAG-binding was expected to entail hydrophobic interactions. To further characterize the interaction of GST-mPIP5K-Iβ with PA, the ability of DAG or PA to compete the binding of GST-mPIP5K-Iβ to PA-coated wells was tested (Fig. 2C). At a concentration of 140 μM,, PA was sufficient to inhibit binding of GST-mPIP5K-Iβ to the immobilized PA by over 90%, suggesting that GST-mPIP5K-Iβ specifically interacts with PA. However, DAG (280 μM) only reduced PA-binding of GST-mPIP5K-Iβ by 40%. This low but reproducible competition by DAG suggests that hydrophobic interactions between GST-mPIP5K-Iβ and the hydrocarbon chains of the acyl groups play a role in the PA binding.

The competition experiments presented above suggested that PA-binding by GST-mPIP5K-Iβ was mediated by both ionic and hydrophobic interactions. To further define the molecular interactions between mPIP5K-Iβ and PA, the GST-PIP5K-Iβ-binding to PA was examined in the presence of sodium pyrophosphate to probe ionic interactions. As shown in Figure 3A, GST-mPIP5K-Iβ-binding to PA was initially diminished when incubated with sodium pyrophosphate at a concentration of 0.83 mM but a much higher concentration of

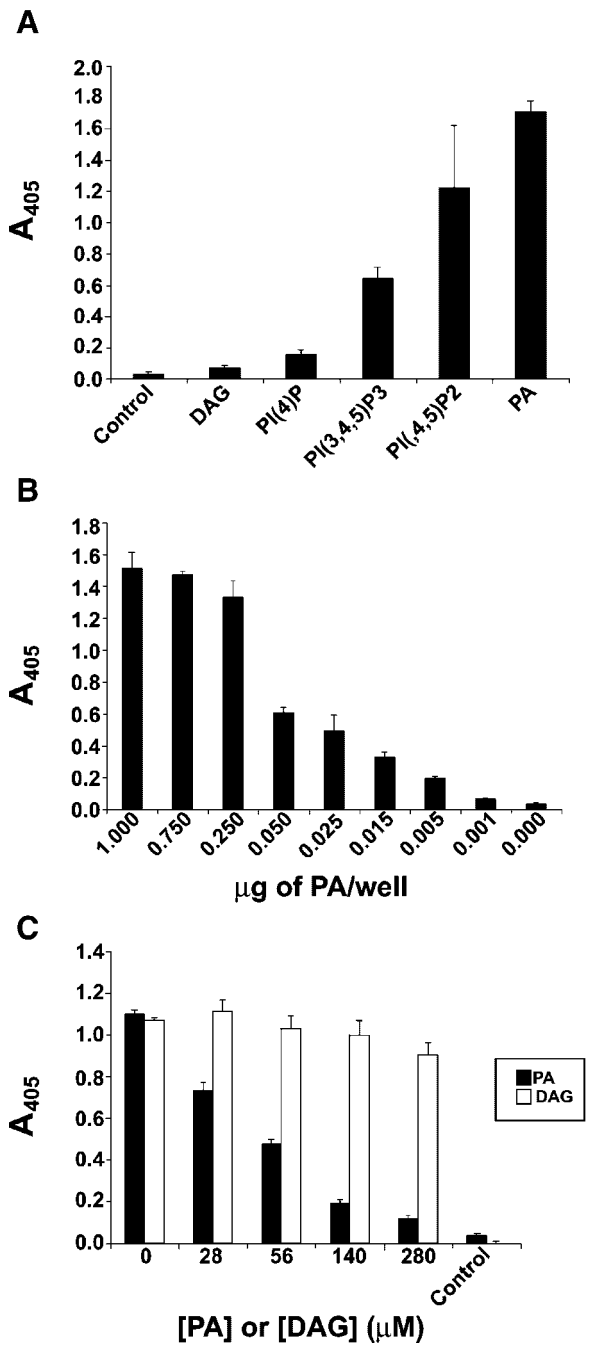

Fig. 2. Specificity of lipid binding to mPIP5K-Iβ. **Panel A** shows the binding of various lipids by GST-mPIP5K-Iβ. Phospholipids were bound to a 96-well microtiter plate (2 μg/well) and the ability of GST-mPIP5K-Iβ to bind to the immobilized lipids was determined using ELISA in which the secondary antibody coupled to alkaline phosphatase. Lipid binding was monitored by an increase in absorbance at 405 nm resulting from the conversion of nitrophenylphosphate (PNPP) to p-nitrophenol. In the control sample, no lipid was bound to the well of the microtiter plate. **Panel B** shows the binding of GST-mPIP5K-Iβ is dependent on the amount of PA bound to the well as determined by the ELISA assay. **Panel C** shows a competition assay in which PA or diacylglycerol (DAG) competes with immobilized PA for binding to GST-mPIP5K-Iβ. In this assay, GST-mPIP5K-Iβ was pre-incubated with either PA or DAG prior to addition to the microtiter plate containing immobilized PA (2 μg/well). The control sample was not pre-incubated with either PA or DAG prior to binding to immobilized PA. In panels A–C, the error bars indicate the standard deviation for three independent experiments.

sodium pyrophosphate (112 mM) was required to achieve a significant decrease in the PA-binding by GST-mPIP5K-Iβ. This biphasic competition suggests that multiple domains of GST-mPIP5K-Iβ may interact with PA through ionic interactions. PA-binding by domain(s) mediated by weaker ionic interactions would be competed at lower relative levels of pyrophosphate while a high affinity domain would be displaced by pyrophosphate only at the highest concentrations.

Hydrophobic interactions mediating binding of GST-mPIP5K-Iβ to PA were further probed by using synthetic PA derivatives prepared with defined acyl chains. As shown in Figure 3B, PA prepared with an acyl chain length of 14 carbons effectively competed with immobilized PA for binding to GST-mPIP5K-Iβ. PA derivatives containing fatty acids of 16 carbon and 18 carbon chains competed GST-mPIP5K-Iβ binding to the immobilized PA, as effectively as, the PA with acyl chain length of 14 carbons (data not shown). However, purified DAG was a more effective competitor of PA-binding by GST-mPIP5K-Iβ than either a PA derivative composed of an eight-carbon chain or lysophophatidic acid. In order to examine the relationship between PA-binding by GST-mPIP5K-Iβ and PA-dependent activation of the kinase activity of GST-mPIP5K-Iβ, the ability of various PA-derivatives to activate the kinase activity of GST-mPIP5K-Iβ purified from 293T cell extracts was determined (Fig. 3C). The synthetic PA-derivatives containing 14-carbons (DMPA), 16-carbons (DPPA), or 18-carbons (DSPA) could compete

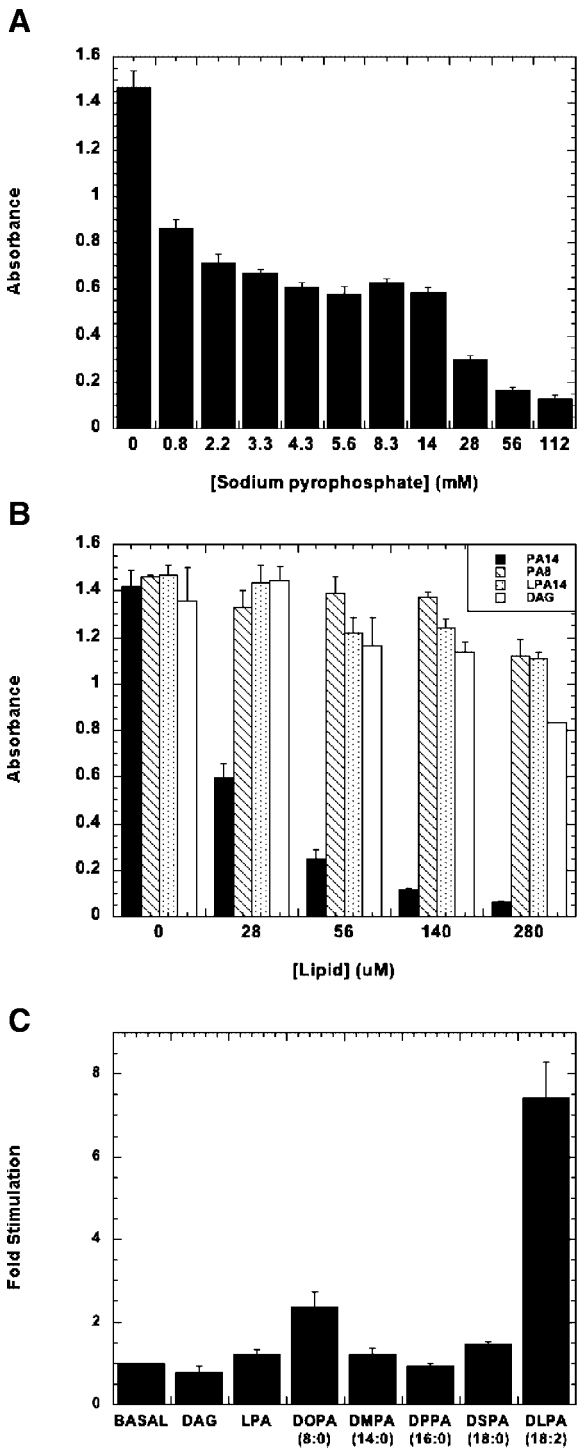

Fig. 3. Characterization of PA binding and activation of PIP5K-Iβ. **Panel A** shows a competition assay in which sodium pyrophosphate was pre-incubated with GST-mPIP5K-Iβ. Binding to immobilized PA was determined using the ELISA assay described in Figure 1. **Panel B** shows a competition assay in which the length of the fatty acid chain or identity of the polar head group is altered. In this assay, lipids were pre-incubated with GST-mPIP5K-Iβ and an ELISA, performed as described in Figure 1, was used to monitor the binding of GST-mPIP5K-Iβ to immobilized PA. Phospholipids used in this experiment are as follows: PA14 is, 2-dimyristoyl-sn-glycero-3-phosphate, PA8 is 1,2-dioctanoyl-sn-glycero-3-phosphate, LPA14 is 1-myristoyl-2-hydroxy-*sn*-glycero-3-phosphate, and DAG is diacylglycerol. **Panel C** shows the activation of GST-mPIP5K-Iβ by phospholipids with varying fatty acid chain lengths and degree of saturation. In this assay, the ability of GST-mPIP5K-Iβ to catalyze the formation of [^{32}P]PI(4,5)P2 from PI(4)P and [^{32}P]-γ-ATP is monitored. The fold stimulation is calculated relative to the activity of GST-mPIP5K-Iβ in the absence of non-substrate phospholipid. Phospholipids used in the assay are as follows: DAG is diacylglycerol; LPA is lysophosphatidic acid, DOPA is 1,2-dioctanoyl-sn-glycero-3-phosphate; DMPA is 1,2-dimyristoyl-sn-glycero-3-phosphate; DPPA 1,2-dipalmityl-sn-glycero-phospahte; DSPA is 1,2, distearoyl-sn-glycero-3-phosphate; DLPA is dilinoleoyl-sn-glycero-3-phosphate, DAPA is 1,2-diarachidonoyl-sn-glycero-3-phosphate. In panels A–C, the error bars indicate the standard deviation for three independent experiments.

for PA-binding by GST-mPIP5K-Iβ, but these molecules failed to activate kinase activity. Interestingly, the incorporation of unsaturated acyl chains into the PA, derivatives resulted in molecules that could strongly activate the kinase activity of GST-mPIP5K-Iβ (DLPA). Since activation of the kinase activity is dependent upon both fatty acid chain length and degree of saturation, the hydrophobic interactions between mPIP5K-Iβ and PA depend on both acyl chain length and degree of fatty acid saturation.

PA Specifically Binds to the C-Terminal Region of mPIP5K-Iβ

Sodium pyrophosphate competed PA-binding by mPIP5K-Iβ in a biphasic manner (Fig. 3A). We hypothesized that this biphasic competition was due to multiple PA-interacting sites within the mPIP5K-Iβ protein that bound PA with differing affinities. To dissect the PA-binding regions within mPIP5K-Iβ, GST-fusion proteins containing the N-terminal (GST-mPIP5K-$I\beta_{1-237}$, $GSTNH_2$) or C-terminal (GST-mPIP5K-$I\beta_{239-546}$, GSTCOOH) of mPIP5K-Iβ were expressed in *E. coli* and affinity purified on glutathione Sepharose. Figure 4A provides a schematic diagram of the different GST-fusion proteins used in this study. Both the N-terminal and the C-terminal regions of mPIP5K-Iβ bound to PA (Fig. 4B). However, GST-mPIP5K-$I\beta_{1-237}$ displayed lower binding to PA than GST-mPIP5K-$I\beta_{239-546}$ or the full-length enzyme, suggesting that the molecular interactions mediating PA-binding to the N-terminal domain were different from those involved in binding the C-terminal domain.

To examine the characteristics of the multiple PA-binding domains within mPIP5K-Iβ, the ability of sodium pyrophosphate or PA to compete the binding of GST-mPIP5K-Iβ, GST-mPIP5K-$I\beta_{1-237}$, and GST-mPIP5K-$I\beta_{239-546}$ to the PA-coated plates was compared. As shown in Figure 4C,D, the binding through the N-terminal domain (GST-mPIP5K-$I\beta_{1-237}$) was competed equally with pyrophosphate and PA, indicating that PA-binding through the N-terminal domain may be mediated primarily by ionic interactions. On the other hand, only 0.25 μmol of PA was required to decrease binding of GST-PIP5K-$I\beta_{239-546}$ by 90%, while 150 μmol of pyrophosphate was required to compete the interaction of the C-terminal domain by an equivalent amount. Therefore, the C-terminal PA-binding domain is likely responsible for the specific high affinity interaction of mPIP5K-Iβ with PA and the NH-terminal domain binds primarily through ionic interactions.

The identification of the C-terminal region as the site of high affinity interactions with PA is not surprising since this region of mPIP5K-Iβ mediates interactions with the phospholipid substrate [Rao et al., 1998; Kunz et al., 2002]. The C-terminal domain of mPIP5K-Iβ interacts with PI(4)P through the activation loop to determine substrate specificity and through the catalytic loop to mediate the catalytic activity of the enzyme. Thus, PA binding to the C-terminal region could activate mPIP5K-Iβ activity via multiple mechanisms. To gain further insight into the mechanism by which PA activates the kinase activity of mPIP5K-Iβ, the C-terminal PA-binding domain of mPIP5K-Iβ was further dissected. Figure 5A provides a schematic diagram of the GST-fusion proteins comprising various regions of the C-terminal region of mPIP5K-Iβ and the relative binding activity of the fusion proteins to PA in the ELISA-based lipid-binding assay is given. Two regions within the C-terminal region of mPIP5K-Iβ displayed PA-binding activity. One region, denoted PA-binding 1 (PAB1), contains the activation loop and the other region, denoted PA-binding 2 (PAB2), contains a region analogous to that proposed to bind PI(4)P in the crystal structure of the type II enzyme [Rao et al., 1998]. Additionally, PAB2 contains the catalytic loop with the catalytic aspartic acid that serves as a weak base involved in the phosphorylation reaction. The binding of the C-terminal region, PAB1, and PAB2 was analyzed as a function of protein concentration (Fig. 5B). The intact C-terminal region displayed the highest affinity binding ($K_m = 15 \pm 2$ nM) and both the individual PAB domains demonstrated binding affinities lower than that of the entire C-terminal region (K_m for PAB1 $= 131 \pm 11$ nM and Km for PAB2 $= 357 \pm 31$ nM). Thus, the high affinity PA-interactions of the C-terminal region may result from cooperation between the domains or the lowered affinities of the isolated domains may result from alterations to the secondary structure of the protein. Thus, high affinity PA-binding by mPIP5K-Iβ is too complex to be fully defined by using this method and will require additional insight into the protein structure of mPIP5K-Iβ.

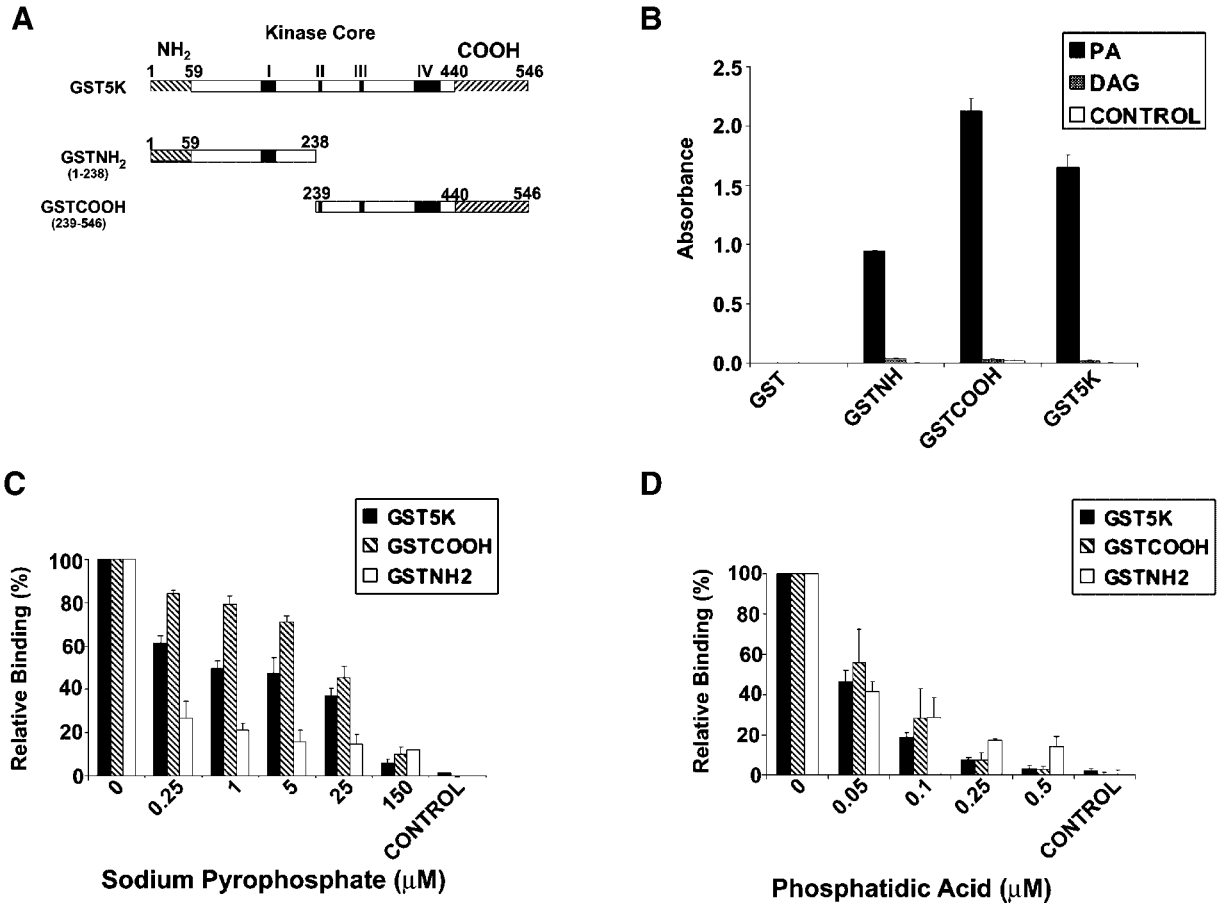

Fig. 4. High affinity PA-binding by bacterially expressed GST-mPIP5K-Iβ is mediated by the C-terminal region of the protein. **Panel A** is a schematic diagram of the regions of mPIP5K-Iβ expressed as GST-fusion proteins. The hatched areas represent the N-terminal and C-terminal regions that are unique between the type I PIP5K isoforms. Regions highly conserved between type I and type II PIP kinases are shown as shaded boxes. Region I corresponds to the ATP binding site, region II corresponds to a putative PI4P-binding site, region III refers to the conserved aspartic acid residue and region IV refers to the activation loop. The amino acid residues for the beginning and ending of each construct are given and are derived from the amino acid for Genbank accession number D86177. **Panel B** shows the PA-binding of the bacterially expressed GST-proteins described in the Panel A. The proteins used in the binding assay are indicated under the bars. Protein binding to PA (dark shaded bars), DAG (light shaded bars) or control (no lipid, open bars) is indicated. The total absorbance of the reactions is given along the Y-axis. **Panels C**, **D** demonstrate that the C-terminal region of mPIP5K-Iβ specifically interacts with PA through ionic and hydrophobic interactions. The ability of sodium pyrophosphate (C), or PA (D) to compete the binding of GST5K, GSTNH2 and GSTCOOH to PA-coated wells was tested. The concentrations of PA (C) and sodium pyrophosphate (D) used in the competition experiments are indicated on the X-axis and the absorbance values are indicated on the Y-axis. PA binding by each of the bacterially expressed proteins was set to 100 and relative binding in the presence of the competitors was calculated. The data shown represent the mean of a triplicate analysis for one representative experiment.

These PA-binding studies suggest that the binding of PA to mPIP5K-Iβ entails multiple domains with the C-terminal region. Further insight into this complexity was provided by examination of the concentration dependent PA-activation of the kinase activity of GST-mPIP5K-Iβ, which was purified from 293T cells (Fig. 5C). Interestingly, the plot of GST-mPIP5K-Iβ enzyme activity as a function of PA concentration produced a sigmoidal curve with a Hill coefficient of 2, strongly suggesting that PA binds cooperatively to mPIP5K-Iβ. While it is not possible to distinguish between cooperative binding of PA to monomeric mPIP5K-Iβ or cooperative binding displayed between monomers of mPIP5K-Iβ dimers or higher order complexes, the observation that the C-terminal region contains multiple PA-binding domains is intriguing.

PA Regulation of mPIP5K-Iβ Kinase Activity

Initial characterization of mPIP5K-Iβ indicated that its activity is stimulated in vitro by PA. To address the question of whether PA

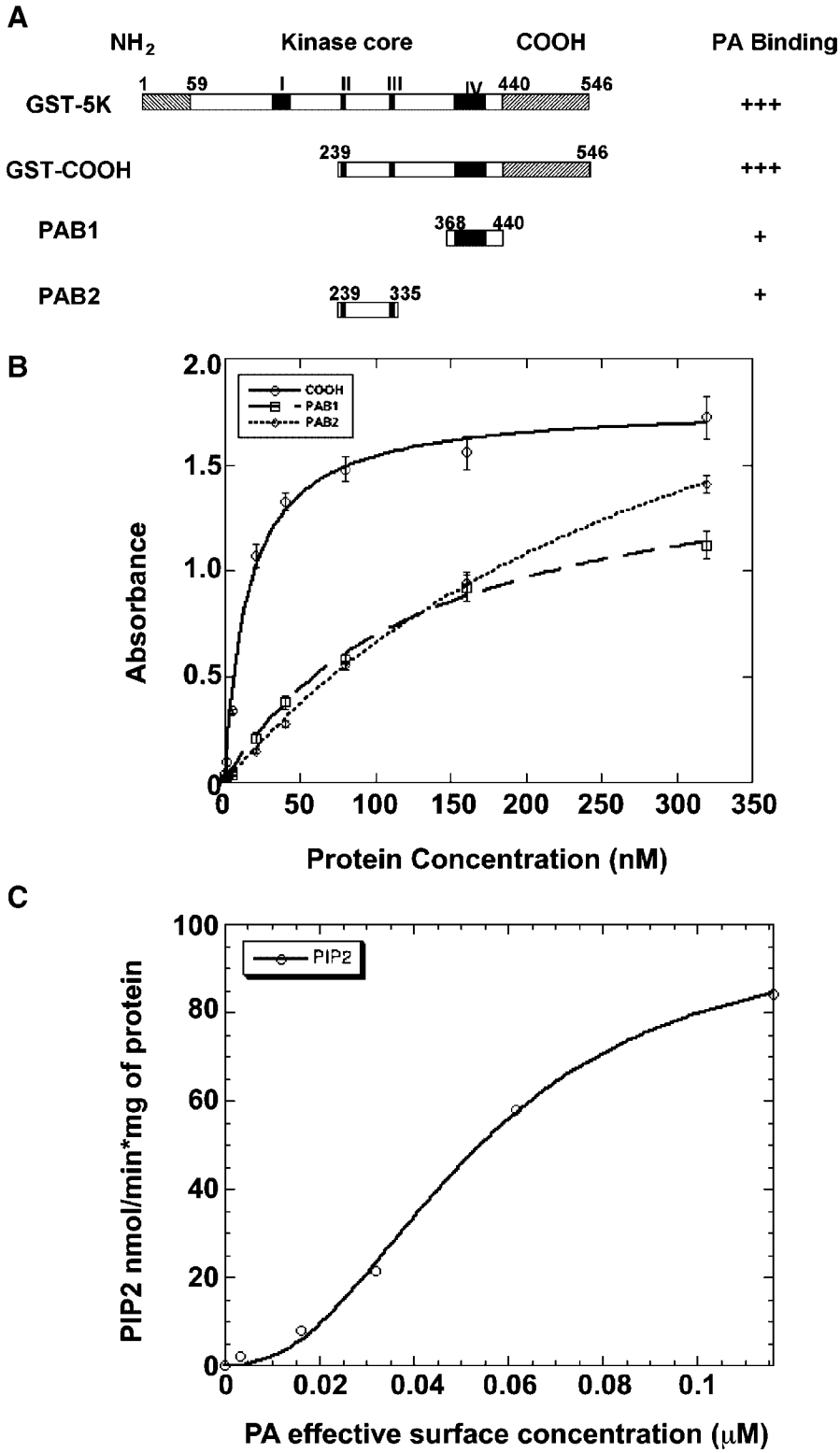

Fig. 5. Two domains within the C-terminal region of mPIP5K-Iβ mediate binding of GST-mPIP5K-Iβ to PA. **Panel A** contains a schematic representation of the regions of mPIP5K-Iβ expressed as GST-fusion proteins in bacteria, purified, and used in the ELISA lipid binding assay. For reference, the full-length protein is shown and annotated as in Figure 4. The N- and C-terminal boundaries of each region of mPIP5K-Iβ expressed as a GST-fusion are given. The ability of each region to bind PA in the ELISA lipid binding assay is indicated by the subjective use of +++ for strong binding and + for modest binding. **Panel B** shows the binding affinity of GST-COOH is higher than either PAB1 or PAB2. The kinetic study of PA-binding by the isolated GST-fusion proteins was performed using the ELISA-based lipid-binding assay with the concentration of GST-fusion proteins shown on the x-axis. **Panel C**: Phosphatidic acid activates the kinase activity of recombinant GST-mPIP5K-Iβ purified from 293T cells with sigmoidal kinetics. Constant amounts of GST-mPIP5K-Iβ were used in in vitro kinase assays employing the various concentrations of PA that are indicated along the X-axis.

regulates the affinity with which PI(4)P binds to mPIP5K-Iβ or the rate at which mPIP5K-Iβ catalyzes the conversion of PI(4)P to PI(4,5)P2, the substrate dependence for the synthesis of PI(4,5)P2 was monitored in the presence and absence of phosphatidic acid under steady state conditions. Like other phospholipids, PI(4)P forms a micelle in the presence of water when its concentration exceeds the critical micelle concentration (CMC). Since mPIP5K-Iβ phosphorylates membrane bound PI(4)P in vivo, it is likely that it also phosphorylates PI(4)P at the surface of the micelle in vitro. Furthermore, although PI(4)P is soluble at concentrations below its CMC, the presence of small aggregates cannot be ruled out. Therefore, kinetic analysis of mPIP5K-Iβ activity over a range of PI(4)P concentrations would be difficult to interpret due to the presence of both soluble PI(4)P and PI(4)P micelles. To overcome this problem, Triton X-100 was used to solubilize all phospholipids. Optimal PA-stimulation of type I PIP5K activity has been previously shown to occur in the presence of Triton X-100 [Moritz et al., 1992; Jenkins et al., 1994].

The rate for PI(4,5)P2 production was determined by monitoring the incorporation of [^{32}P]ATP into PI(4)P. A plot of the initial rate versus the total concentration of PI(4)P exhibits sigmoidal kinetics (Fig. 6A). In addition, above 150 μM PI(4)P, there is a decrease in the initial rate, suggesting the presence of substrate inhibition. Attempts to fit the experimental data to a modified Hill equation that incorporates uncompetitive substrate inhibition were unsuccessful both in the absence and the presence of PA, (Fig. 6, Panels A and B). Similarly, attempts to fit the data to a Hill equation that incorporates noncompetitive substrate inhibition were also unsuccessful (data not shown). The inability of the direct binding model to account for the observed kinetics led us to consider the possibility that catalysis of PI(4)P phosphorylation follows the surface dilution kinetics model proposed by Hendrickson and Dennis [Hendrickson and Dennis, 1984]. In this model, there is an initial nonspecific binding of the enzyme to the surface of the micelle, followed by the specific binding of the phospholipid substrate. It is assumed that there is a rapid equilibrium between protein in solution and protein bound to the micelle. The rate of catalysis depends on the ability of the enzyme to bind substrate after it has bound to the micelle. In other words, it is the effective concentration of the substrate at the surface of the micelle, not the total substrate concentration that determines the rate. The effective concentration of PI(4)P at the surface of the micelle was calculated according to Equation 5 and the initial rate of PI(4,5)P2 production versus the effective concentration of PI(4)P ([PI(4)P$_e$]) was plotted. The data were fit to a modified Michaelis–Menten equation that

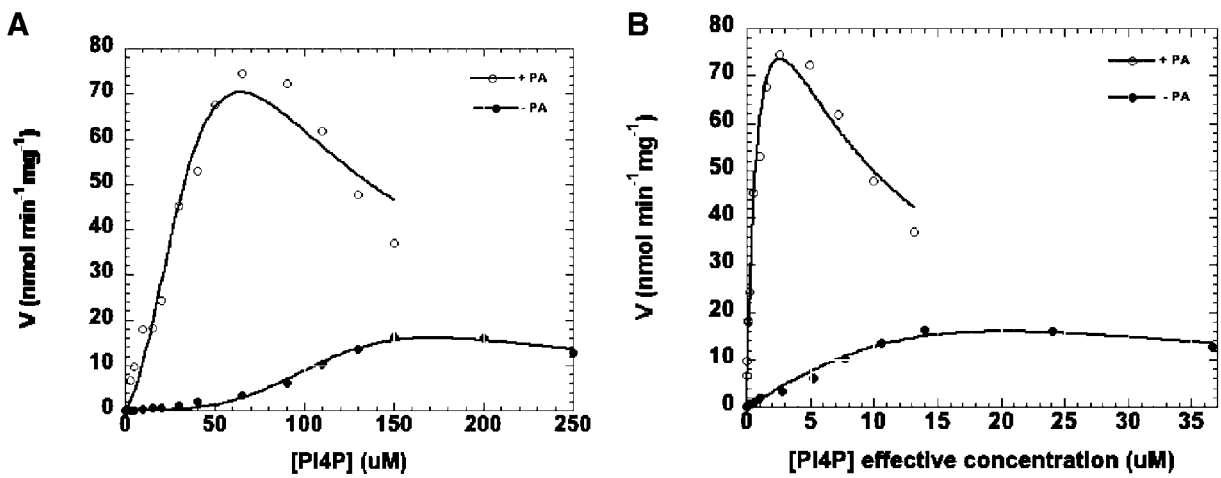

Fig. 6. PA increases the affinity of mPIP5K-Iβ for PI(4)P. The activity of mPIP5K-Iβ towards PI(4)P/Triton X-100 mixed micelles was determined in the absence (filled circles) and presence (open circles) of 100 μM PA. In **Panel A**, the data are fit to a Hill equation, where the enzyme is assumed to initially interact directly with the PI(4)P substrate (eq. 1). The concentration of [PI(4)P] corresponds to the total concentration of PI(4)P. In **Panel B**, the data are fit to a model in which the enzyme is assumed to initially bind to the lipid micelle, then subsequently bind the PI(4)P substrate (Eq. 2). In this model, the concentration of PI(4)P corresponds to its concentration in the lipid micelle (i.e., the effective concentration).

incorporates uncompetitive substrate inhibition (Eq. 2). This model produced a curve that fit the data points except at the highest substrate concentrations. Although the calculations based on this model must be interpreted cautiously due to variation at high PI(4)P concentrations, it appears that the addition of PA to the reaction increases the affinity for the binding of PI(4)P to the active site of mPIP5K-Iβ by nearly 70-fold (Fig. 6B, Table I). In contrast, PA appears to have little effect on the affinity with which PI(4)P binds to the inhibitory site on PIP5K-Iβ (Table I). Similarly, the PA does not appear to significantly alter the k_{cat} for the enzyme (Table I).

DISCUSSION

In addition to its canonical role as the precursor of the second messengers diacylglycerol and inositol-(1,3,5)-trisphosphate, PI(4,5)P2 is known to regulate the activity and localization of proteins involved in actin polymerization, vesicle trafficking, and endocytosis. Coordination of these signaling events requires both temporal and spatial regulation of PI(4,5)P2 synthesis. Although, it has been shown that PIP5KI activity is stimulated by phosphatidic acid in vitro, the mechanism of phosphatidic acid-mediated regulation of PIP5K-Iβ activity or its role in the spatial and temporal regulation of PI(4,5)P2 synthesis has not been determined.

Previous work clearly implicated PA and PI(4,5)P2 in the regulation of actin polymerization [Cross et al., 1996; Shibasaki et al., 1997; Ishihara et al., 1998; Rozelle et al., 2000]and this present study suggests that phospholipase D and PIP5Ks act in a common pathway to regulate actin stress fiber formation. This conclusion is supported by evidence of an interdependent relationship between PA production by phospholipase D isoforms and PI(4,5)P2 production by the type I PIP5Ks in the regulation of endocytosis and in response to the small G-protein ARF6 [Arneson et al., 1999; Divecha et al., 2000]. Since, type I PIP5K activity is stimulated by PA and PI(4,5)P2 activates phospholipase D, a positive feedback loop is potentially formed between these enzyme families. In support of these observations, recent studies in *Dictyostelium* identified a requirement of phospholipase D production of PA for the regulation of the actin cytoskeleton and linked PA production to PI(4,5)P2 synthesis [Zouwail et al., 2005]. Thus, the observation that PA regulates type I PIP5K activity to control actin stress fiber formation in NIH 3T3 cells provides substantiating evidence for this interdependent relationship between phospholipase D and type I PIP5Ks.

TABLE I. Kinetic Parameters of mPIP5KI-β[a]

	$K_d^{PA(4)P_e}$	$K_i^{PA(4)P_e}$	k_{cat}
	μM	μM	min^{-1}
− PA	134 (± 5)	2.4 (± 0.5)	16.4 (± 0.6)
+ PA	2.0 (± 0.5)	4.2 (± 0.8)	17 (± 1)

[a]The standard deviations for three independent experiments are indicated in parentheses.

Since the identification of PA as a potent activator of the type I PIP5Ks [Moritz et al., 1992; Jenkins et al., 1994], studies of the PA-dependent activation of PIP5Ks have concentrated more on cell biology and less on biochemistry. PA binding by mPIP5K-Iβ employs both electrostatic and hydrophobic interactions. Such complex interactions are not surprising since the crystal structure of the related type II PIP kinase suggests that membrane interactions are mediated by electrostatic interactions over a large face of the protein [Rao et al., 1998]. Hydrophobic interactions with PA not only determine the ability of mPIP5K-Iβ to bind the lipid but also the ability of the lipid to activate mPIP5K-Iβ kinase activity. While PA derivatives containing fatty acids composed of 14 carbons or longer are sufficient to bind mPIP5K-Iβ, efficient activation of mPIP5K-Iβ kinase activity also required that the fatty acids are unsaturated. Interestingly, PA generated by phospholipase D activity in vivo predominantly contains monounsaturated and di-unsaturated fatty acids [Pettitt et al., 2001]. Thus, the PA-binding and activation of mPIP5K-Iβ observed in our studies reflects the structure of PA generated in vivo.

Few PA-binding domains have been identified and mPIP5K-Iβ does not display sequence similarities to proteins with defined PA-binding domains. Two PA-binding domains (PAB1 and PAB2) were identified within the C-terminal domain. Both domains were associated with areas implicated in substrate binding, PAB1 fell within the activation loop and PAB2 contains regions implicated in PI(4)P binding and catalysis inferred from the crystal structure of the related type II PIP kinase [Rao et al., 1998].

However, the isolated PA-binding domains displayed binding affinities much lower than the full C-terminal region suggesting that high affinity interactions require secondary structure features inherent to a properly folded protein. Thus, further dissection of the mPIP5K-Iβ PA-binding domain will require more sophisticated analysis of the structure of the protein.

Analysis of the effect of PA on PIP5K-Iβ activity is complicated by both the sigmoidal nature of enzyme activity with respect to total concentration of PI(4)P and the inhibition of PIP5K-Iβ activity by the substrate of the reaction, PI(4)P. The sigmoidicity for the [PI(4)P] versus initial rate plot is eliminated when the effective concentration of PI(4)P is used in place of the total concentration of PI(4)P. These results are consistent with mPIP5K-Iβ following the surface dilution model described by Hendrickson and Dennis in which the enzyme initially binds to the micelle in a nonspecific manner, then subsequently binds the substrate of the reaction [Hendrickson and Dennis, 1984]. In this model, the rate at which the enzyme binds substrate is dependent on the concentration of the substrate in the micelle (i.e., the effective concentration), not the total concentration of substrate in solution (since the enzyme only binds substrate after it is bound to the micelle). The inhibition of PIP5K-Iβ activity at high substrate concentrations can be explained using an uncompetitive inhibition model in which the substrate of the reaction, PI(4)P, also inhibits the enzyme. Although there are some discrepancies at high PI(4)P concentrations, the uncompetitive inhibition model fits the data reasonably well.

The inhibition of mPIP5K-Iβ by the PI(4)P substrate is consistent with a model which there are two binding sites for PI(4)P in PIP5K-Iβ, one of which inhibits the rate at which the active site catalyzes the conversion of PI(4)P to PI (4,5)P2. However, this model does not distinguish between inhibition arising from the presence of an inhibitory binding site in the mPIP5K-Iβ monomer and inhibition mediated by PI(4)P binding to the catalytic site on the monomer. Crystallographic studies of the related type II phosphatidylinositol phosphate kinase suggest that mPIP5K-Iβ is dimeric with the monomers oriented such that the active site of one monomer faces the membrane and the active site of the other monomer is solvent exposed [Rao et al., 1998]. This is consistent with functional analysis of the conserved domains, which suggest that mPIP5K-Iβ contains multiple dimerization domains [Galiano et al., 2002]. Thus, substrate binding to one catalytic site on the dimer could result in inhibition of the other catalytic site. Identification of the mechanism of substrate inhibition will require additional studies aimed at defining PI(4)P binding sites in mPIP5K-Iβ and structural studies to define the effects of substrate binding on the structure of the mPIP5K-Iβ dimer.

Although PA appears to affect the V_{max} of mPIP5K-Iβ, analysis of the K_m and k_{cat} values indicates that phosphatidic acid exerts its effects by increasing the affinity of the active site for PI(4)P and not through changes in the k_{cat} value. The apparent decrease in V_{max} is actually due to substrate inhibition by PI(4)P. In the absence of PA, the inhibitory constant is 50-fold smaller than the Michaelis constant for PI(4)P ($K_i^{PI(4)P} = 2.4$ μM vs. $K_m^{PI(4)P} = 134$ μM). As a result, even at low substrate concentrations, when the enzyme has little PI(4)P bound to the active site, there is a significant amount of substrate inhibition. For example, at 5 mM PI(4)P, only 3.6% of the active site has substrate bound to it, while 68% of the inhibitory binding site contains bound substrate. The addition of PA increases the affinity with which the active site of mPIP5K-Iβ binds PI(4)P by 67-fold. This results in a larger proportion of the enzyme containing PI(4)P bound at the active site at low substrate concentrations. In addition, the affinity with which PI(4)P binds to the inhibitory site is decreased almost twofold by PA. The combination of these factors result in the increased activity observed for mPIP5K-Iβ at low concentrations of PI(4)P when PA is present. For example, at 5 mM PI(4)P, in the presence of PA, approximately 70% of the active site will contain bound substrate, while only 54% of the inhibitory site will contain PI(4)P.

While PA activation of mPIP5K-Iβ has been observed, this study is the first attempt to describe the mechanism through which PA acts. In the course of these studies, we provide evidence that mPIP5K-Iβ binds substrate through a surface dilution kinetic model and that mPIP5K-Iβ displays substrate inhibition. Although limited analyses of the type I PIP5K enzyme kinetics have been performed, previous studies have failed to identify these attributes of

type I PIP5K activity. The studies described in this report were performed over a broad range of substrate concentrations allowing the substrate dependence of mPIP5K-Iβ activity to be more fully elucidated.

The substrate inhibition exhibited by mPIP5K-Iβ has potential biological consequences. In particular, inhibition of mPIP5K-Iβ by PI(4)P may provide a convenient mechanism for regulating PI(4,5)P2 production. Numerous studies have defined enrichment of phosphoinositdes in discrete microdomains [Botelho et al., 2000; Rozelle et al., 2000; Bodin et al., 2001; Caroni, 2001; Marshall et al., 2001; Miaczynska and Zerial, 2002; Zhuang et al., 2002]. Localization of PI to membrane rafts and other microdomains may be protein mediated or a characteristic of PI since phosphatidylinositol monophosphates will form microdomains spontaneously in vitro [Redfern and Gericke, 2004]. One consequence of the microdomains is that the PI-modifying enzymes are exposed to high local substrate concentrations. Thus, substrate inhibition represents a mechanism to limit the activity of mPIP5K-Iβ in the unstimulated state**.** In this scenario, mPIP5K-Iβ is primed to transmit an intracellular signal (through the production of PI(4,5)P2) but is held in check until an activating signal such as an increase in PA occurs. In effect, substrate inhibition allows the enzyme to be literally surrounded by substrate, yet unable to efficiently process it until the activating signal is received.

ACKNOWLEDGMENTS

The authors thank Dr. Shari Meyers for the critical reading of the manuscript and Dr. Kelly Tachell for the generous use of the microscope imaging system. Additional support was provided by the Feist-Weiller Cancer Center.

REFERENCES

Aikawa Y, Martin TF. 2003. ARF6 regulates a plasma membrane pool of phosphatidylinositol(4,5)bisphosphate required for regulated exocytosis. J Cell Biol 162:647–659.

Arneson LS, Kunz J, Anderson RA, Traub LM. 1999. Coupled inositide phosphorylation and phospholipase D activation initiates clathrin-coat assembly on lysosomes. J Biol Chem 274:17794–17805.

Barbieri MA, Heath CM, Peters EM, Wells A, Davis JN, Stahl PD. 2001. Phosphatidylinositol-4-phosphate 5-kinase-1beta is essential for epidermal growth factor receptor-mediated endocytosis. J Biol Chem 276:47212–47216.

Bodin S, Giuriato S, Ragab J, Humbel BM, Viala C, Vieu C, Chap H, Payrastre B. 2001. Production of phosphatidylinositol 3,4,5-trisphosphate and phosphatidic acid in platelet rafts: evidence for a critical role of cholesterol-enriched domains in human platelet activation. Biochemistry 40:15290–15299.

Boronenkov IV, Loijens JC, Umeda M, Anderson RA. 1998. Phosphoinositide signaling pathways in nuclei are associated with nuclear speckles containing pre-mRNA processing factors. Mol Biol Cell 9:3547–3560.

Botelho RJ, Teruel M, Dierckman R, Anderson R, Wells A, York JD, Meyer T, Grinstein S. 2000. Localized biphasic changes in phosphatidylinositol-4,5-bisphosphate at sites of phagocytosis. J Cell Biol 151:1353–1368.

Brown FD, Rozelle AL, Yin HL, Balla T, Donaldson JG. 2001. Phosphatidylinositol 4,5-bisphosphate and Arf6-regulated membrane traffic. J Cell Biol 154:1007–1017.

Caroni P. 2001. New EMBO members' review: Actin cytoskeleton regulation through modulation of PI (4,5)P(2) rafts. EMBO J 20:4332–4336.

Chatah NE, Abrams CS. 2001. G-protein-coupled receptor activation induces the membrane translocation and activation of phosphatidylinositol-4-phosphate 5-kinase I alpha by a Rac- and Rho-dependent pathway. J Biol Chem 276:34059–34065.

Chen C, Okayama H. 1987. High-efficiency transformation of mammalian cells by plasmid DNA. Mol Cell Biol 7:2745–2752.

Cross MJ, Roberts S, Ridley AJ, Hodgkin MN, Stewart A, Claesson-Welsh L, Wakelam MJ. 1996. Stimulation of actin stress fibre formation mediated by activation of phospholipase D. Curr Biol 6:588–597.

Davis JN, Rock CO, Cheng M, Watson JB, Ashmun RA, Kirk H, Kay RJ, Roussel MF. 1997. Complementation of growth factor receptor-dependent mitogenic signaling by a truncated type I phosphatidylinositol 4-phosphate 5-kinase. Mol Cell Biol 17:7398–7406.

Di Paolo G, Pellegrini L, Letinic K, Cestra G, Zoncu R, Voronov S, Chang S, Guo J, Wenk MR, De Camilli P. 2002. Recruitment and regulation of phosphatidylinositol phosphate kinase type 1 gamma by the FERM domain of talin. Nature 420:85–89.

Di Paolo G, Moskowitz HS, Gipson K, Wenk MR, Voronov S, Obayashi M, Flavell R, Fitzsimonds RM, Ryan TA, De Camilli P. 2004. Impaired PtdIns(4,5)P2 synthesis in nerve terminals produces defects in synaptic vesicle trafficking. Nature 431:415–422.

Divecha N, Roefs M, Halstead JR, D'Andrea S, Fernandez-Borga M, Oomen L, Saqib KM, Wakelam MJ, D'Santos C. 2000. Interaction of the type Ialpha PIPkinase with phospholipase D: A role for the local generation of phosphatidylinositol 4, 5-bisphosphate in the regulation of PLD2 activity. EMBO J 19:5440–5449.

Doughman RL, Firestone AJ, Anderson RA. 2003a. Phosphatidylinositol phosphate kinases put PI4,5P(2) in its place. J Membr Biol 194:77–89.

Doughman RL, Firestone AJ, Wojtasiak ML, Bunce MW, Anderson RA. 2003b. Membrane ruffling requires coordination between type Ialpha phosphatidylinositol phosphate kinase and Rac signaling. J Biol Chem 278:23036–23045.

Galiano FJ, Ulug ET, Davis JN. 2002. Overexpression of murine phosphatidylinositol 4-phosphate 5-kinase type

Ibeta disrupts a phosphatidylinositol 4,5 bisphosphate regulated endosomal pathway. J Cell Biochem 85: 131–145.

Ghosh S, Strum JC, Sciorra VA, Daniel L, Bell RM. 1996. Raf-1 kinase possesses distinct binding domains for phosphatidylserine and phosphatidic acid. Phosphatidic acid regulates the translocation of Raf-1 in 12-O-tetradecanoylphorbol-13-acetate-stimulated Madin-Darby canine kidney cells. J Biol Chem 271: 8472–8480.

Hendrickson HS, Dennis EA. 1984. Kinetic analysis of the dual phospholipid model for phospholipase A2 action. J Biol Chem 259:5734–5739.

Honda A, Nogami M, Yokozeki T, Yamazaki M, Nakamura H, Watanabe H, Kawamoto K, Nakayama K, Morris AJ, Frohman MA, Kanaho Y. 1999. Phosphatidylinositol 4-phosphate 5-kinase alpha is a downstream effector of the small G protein ARF6 in membrane ruffle formation. Cell 99:521–532.

Ishihara H, Shibasaki Y, Kizuki N, Katagiri H, Yazaki/ SNM> Y, Asano T, Oka Y. 1996. Cloning of cDNAs encoding two isoforms of 68-kDa type I phosphatidylinositol-4-phosphate 5-kinase. J Biol Chem 271:23611–23614.

Ishihara H, Shibasaki Y, Kizuki N, Wada T, Yazaki Y, Asano T, Oka Y. 1998. Type I phosphatidylinositol-4-phosphate 5-kinases. Cloning of the third isoform and deletion/substitution analysis of members of this novel lipid kinase family. J Biol Chem 273:8741–8748.

Itoh T, Ijuin T, Takenawa T. 1998. A novel phosphatidylinositol-5-phosphate 4-kinase (phosphatidylinositol-phosphate kinase IIgamma) is phosphorylated in the endoplasmic reticulum in response to mitogenic signals. J Biol Chem 273:20292–20299.

Jenkins GH, Fisette PL, Anderson RA. 1994. Type I phosphatidylinositol 4-phosphate 5-kinase isoforms are specifically stimulated by phosphatidic acid. J Biol Chem 269:11547–11554.

Kam Y, Exton JH. 2001. Phospholipase D activity is required for actin stress fiber formation in fibroblasts. Mol Cell Biol 21:4055–4066.

Kunz J, Fuelling A, Kolbe L, Anderson RA. 2002. Stereospecific substrate recognition by phosphatidylinositol phosphate kinases is swapped by changing a single amino acid residue. J Biol Chem 277:5611–5619.

Ling K, Doughman RL, Firestone AJ, Bunce MW, Anderson RA. 2002. Type I gamma phosphatidylinositol phosphate kinase targets and regulates focal adhesions. Nature 420:89–93.

Loijens JC, Anderson RA. 1996. Type I phosphatidylinositol-4-phosphate 5-kinases are distinct members of this novel lipid kinase family. J Biol Chem 271:32937–32943.

Loijens JC, Boronenkov IV, Parker GJ, Anderson RA. 1996. The phosphatidylinositol 4-phosphate 5-kinase family. Adv Enzyme Regul 36:115–140.

Marshall JG, Booth JW, Stambolic V, Mak T, Balla T, Schreiber AD, Meyer T, Grinstein S. 2001. Restricted accumulation of phosphatidylinositol 3-kinase products in a plasmalemmal subdomain during Fc gamma receptor-mediated phagocytosis. J Cell Biol 153:1369–1380.

Miaczynska M, Zerial M. 2002. Mosaic organization of the endocytic pathway. Exp Cell Res 272:8–14.

Moritz A, De Graan PN, Gispen WH, Wirtz KW. 1992. Phosphatidic acid is a specific activator of phosphatidylinositol-4-phosphate kinase. J Biol Chem 267:7207–7210.

Oude Weernink PA, Schmidt M, Jakobs KH. 2004. Regulation and cellular roles of phosphoinositide 5-kinases. Eur J Pharmacol 500:87–99.

Park SJ, Itoh T, Takenawa T. 2001. Phosphatidylinositol 4-phosphate 5-kinase type I is regulated through phosphorylation response by extracellular stimuli. J Biol Chem 276:4781–4787.

Pettitt TR, McDermott M, Saqib KM, Shimwell N, Wakelam MJ. 2001. Phospholipase D1b and D2a generate structurally identical phosphatidic acid species in mammalian cells. Biochem J 360:707–715.

Rao VD, Misra S, Boronenkov IV, Anderson RA, Hurley JH. 1998. Structure of type IIbeta phosphatidylinositol phosphate kinase: A protein kinase fold flattened for interfacial phosphorylation. Cell 94:829–839.

Redfern DA, Gericke A. 2004. Domain formation in phosphatidylinositol monophosphate/phosphatidylcholine mixed vesicles. Biophys J 86:2980–2992.

Rozelle AL, Machesky LM, Yamamoto M, Driessens MH, Insall RH, Roth MG, Luby-Phelps K, Marriott G, Hall A, Yin HL. 2000. Phosphatidylinositol 4,5-bisphosphate induces actin-based movement of raft-enriched vesicles through WASP-Arp2/3. Curr Biol 10:311–320.

Shibasaki Y, Ishihara H, Kizuki N, Asano T, Oka Y, Yazaki Y. 1997. Massive actin polymerization induced by phosphatidylinositol-4-phosphate 5-kinase in vivo. J Biol Chem 272:7578–7581.

Skippen A, Jones DH, Morgan CP, Li M, Cockcroft S. 2002. Mechanism of ADP ribosylation factor-stimulated phosphatidylinositol 4,5-bisphosphate synthesis in HL60 cells. J Biol Chem 277:5823–5831.

Wang YJ, Li WH, Wang J, Xu K, Dong P, Luo X, Yin HL. 2004. Critical role of PIP5KI{gamma}87 in InsP3-mediated Ca(2+) signaling. J Cell Biol 167:1005–1010.

Weernink PA, Meletiadis K, Hommeltenberg S, Hinz M, Ishihara H, Schmidt M, Jakobs KH. 2004. Activation of type I phosphatidylinositol 4-phosphate 5-kinase isoforms by the Rho GTPases, RhoA, Rac1, and Cdc42. J Biol Chem 279:7840–7849.

Wenk MR, Pellegrini L, Klenchin VA, Di Paolo G, Chang S, Daniell L, Arioka M, Martin TF, De Camilli P. 2001. PIP kinase Igamma is the major PI(4,5)P(2) synthesizing enzyme at the synapse. Neuron 32:79–88.

Yang SA, Carpenter CL, Abrams CS. 2004. Rho and Rho-kinase mediate thrombin-induced phosphatidylinositol 4-phosphate 5-kinase trafficking in platelets. J Biol Chem 279:42331–42336.

Yin HL, Janmey PA. 2003. Phosphoinositide regulation of the actin cytoskeleton. Annu Rev Physiol 65:761–789.

Zhuang L, Lin J, Lu ML, Solomon KR, Freeman MR. 2002. Cholesterol-rich lipid rafts mediate akt-regulated survival in prostate cancer cells. Cancer Res 62:2227–2231.

Zouwail S, Pettitt TR, Dove SK, Chibalina MV, Powner DJ, Haynes L, Wakelam MJ, Insall RH. 2005. Phospholipase D activity is essential for actin localization and actin-based motility in Dictyostelium. Biochem J 389:207–214.